Pretreatment With Propofol Restores Intestinal Epithelial Cells Integrity Disrupted by Mast Cell Degranulation *in vitro*

Jinfei LI[1,2#], **Jingxia HUANG**[1#], **Rui ZHANG**[1], **Yiquan LIN**[1], **Qianru CHEN**[1], **Xiaoliang GAN**[1]

[#]*These authors contributed equally to this work*

[1]Department of Anesthesiology, State Key Laboratory of Ophthalmology, Zhongshan Ophthalmic Center, Sun Yat-sen University, China, [2]Department of Anesthesiology, Guangdong Women and Children Hospital, China

Summary

Propofol has been shown to against intestinal reperfusion injury when treated either before or after ischemia, during which mast cell could be activated. The aim of this study was to evaluate the role of propofol in restoring the intestinal epithelial cells integrity disrupted by mast cell activation or the released tryptase after activation *in vitro*. We investigated the effect of: (1) tryptase on Caco-2 monolayers in the presence of PAR-2 inhibitor or propofol, (2) mast cell degranulation in a Caco-2/LAD-2 co-culture model in the presence of propofol, and (3) propofol on mast cell degranulation. Epithelial integrity was detected using transepithelial resistance (TER) and permeability to fluorescein isothiocyanate (FITC)-dextran (the apparent permeability coefficient, Papp). The expression of junctional proteins zonula occludens-1 (ZO-1/TJP1) and occludin were determined using western blot analysis and immunofluorescence microscopy. The intracellular levels of reactive oxidative species (ROS) and Ca^{2+} were measured using flow cytometry. Tryptase directly enhanced intestinal barrier permeability as demonstrated by significant reductions in TER, ZO-1, and occludin protein expression and concomitant increases in Papp. The intestinal barrier integrity was restored by PAR-2 inhibitor but not by propofol. Meanwhile, mast cell degranulation resulted in epithelial integrity disruption in the Caco-2/LAD-2 co-culture model, which was dramatically attenuated by propofol. Mast cell degranulation caused significant increases in intracellular ROS and Ca^{2+} levels, which were blocked by propofol and NAC. Propofol pretreatment can inhibit mast cell activation via ROS/Ca^{2+} and restore the intestinal barrier integrity induced by mast cell activation, instead of by tryptase.

Corresponding author

Xiaoliang Gan, Department of Anesthesiology, State Key Laboratory of Ophthalmology, Zhongshan Ophthalmic Center, Sun Yat-sen University. Email: ganxl@mail.sysu.edu.cn

Introduction

Intestinal barrier plays critical roles in maintaining gut hemostasis [1], and disruption of the barrier induces bacteria translocation in many clinical conditions including hemorrhagic shock. The pathophysiologic changes result in systemic inflammatory syndrome (SIRS) and even multiple organs failure [2].

The number of mast cells, mainly located in the human gastrointestinal tract, are strongly associated with intestinal transcellular permeability in IBS patients [3,4]. Mast cell activation can be initiated during the period of ischemia, and many mediators can be secreted from mast cell activation. Of the mediators, tryptase accounts for one fourth of the released proteins and directly induces intestinal epithelial injury via protease-activated receptor (PAR)-2/ERK *in vitro* [5].

Propofol is one of usually used intravenous anesthetics for anesthesia. Besides the anesthesia effects, it has been demonstrated to attenuate ischemia reperfusion injury in many studies due to its antioxidative

properties [6], further, previous study revealed that propofol can inhibit mast cell exocytosis [7], our previous study demonstrated that pretreatment with propofol can protect the intestines against mast cell activation-exacerbated ischemia reperfusion injury [6], implying propofol pretreatment could restore intestinal barrier integrity disrupted by mast cell degranulation. Meanwhile, propofol has been shown to exert anti-proinflammatory properties via ERK down-regulating [8], suggesting the therapeutic benefits of post-treatment with propofol against tryptase-induced intestinal barrier integrity disruption after mast cell degranulation.

Based on the previous findings, we hypothesized that underlying mechanisms by which preconditioning or postconditioning with propofol in restoring intestinal barrier integrity may through mast cells stabilization or blocking tryptase respectively. The hypothesis was tested in the human intestinal epithelial cell line Caco-2 challenged by tryptase stimulation or mast cell degranulation in the presence or absence of *in vitro* propofol treatment.

Materials and Methods

Materials and reagents were purchased form KeyGEN BioTech (Nanjing, China) unless stated otherwise.

Cell culture

The human colon adenocarcinoma cell line, Caco-2, was cultured in Dulbecco's modified Eagle's Medium with 10 %. v/v fetal bovine serum (PAN-Seratech, Aidenbach, Germany) and 5 %. CO_2 (37 °C). Cells were cultured in 75 cm^2 tissue culture flasks until high density before seeding on Transwell® polyester filters (0.4 μm. Corning, NY, USA) in 6-well plates (Corning, NY, USA), or EZSlide 8-well glass slides (Merck Millipore, Burlington, USA). Cells on Transwell filters were cultivated for 21 days to form monolayers.

The human mast cell line, LAD-2, was purchased from Otwo Biotech (Guangzhou, China). LAD-2 cells (P20 to P50) were cultured in Iscove's modified Dulbecco's Medium with 10 %. v/v fetal bovine serum and 5 %. CO_2 (37 °C). Cells were cultured in 75 cm^2 tissue culture flasks, passaged approximately once a week, and seeded in 6-well plates for experiments or the basolateral compartment of Transwells.

The mouse mast cell line, MC-9, was also purchased from Otwo Biotech (Guangzhou, China). MC-9 cells (P20 to P50) were cultured in Dulbecco's

modified Eagle's Medium with 10 %. v/v fetal bovine serum and 5 %. CO_2 (37 °C). Cells were cultured in 75 cm^2 tissue culture flasks, passaged approximately once a week, and seeded in 6-well plates for experiments.

Co-culture of Caco-2 and LAD-2 cells: Caco-2 cells were seeded on Transwell filters with a density 5×10^5 cells /ml in Dulbecco's modified Eagle's medium with 10 %. v/v fetal bovine serum until the 20th day. LAD-2 cells (5×10^5 cells /ml) were added to the basolateral compartment of the Transwells in Iscove's modified Dulbecco's Medium with 10 %. v/v fetal bovine serum (5 %. CO_2, 37 °C). Caco-2 cells were also cultured without LAD-2 cells as controls.

When the cell culture was completed, model intervention could be performed. Tryptase (10/100/1000ng/ml), FS (PAR2 inhibitor, 100μM), propofol (50/10/1μM), A23187 (calcium ionophore, 1/5/10μM), NAC (ROS scavenger, 1:250) was added to the basolateral compartment of the Transwells according to the plan and incubated for 4h or 24h.

Integrity and paracellular permeability of Caco-2 monolayers

Caco-2 monolayer integrity was determined with transepithelial resistance (TER) measured with an epithelial volt-ohm meter, Millicell® ERS-2 (Merck Millipore, Burlington, USA). TER was measured once every two days from the 7th to the 20th day to confirm Caco-2 monolayer formation. The results were displayed as a percentage change over the untreated control. To determine epithelial permeability, FITC-dextran (4 kDa, 100 μg/ml) was added to the apical compartment of Transwells after washing with Hank's balanced salt solution (HBSS) four times. Basolateral samples were taken at 30 min and 60 min before replenishing with fresh HBSS after each sampling. The apical-to-basolateral flux of FITC-dextran from 30 to 60 min was measured with a microplate spectrophotometer (BioTek, Winooski, Vermont, USA) using an external standard curve. The apparent permeability coefficient (Papp) was calculated according to Papp = dQ/dt (1/AC0), where dQ/dt is the permeability rate, A is the crossing area, and C0 is the initial donor solution concentration [9].

Western blotting of TJ proteins expression

Monolayers of Caco-2 cells in 6-well plates were lysed in cold RIPA buffer (Beyotime, Shanghai, China) with protease inhibitor cocktail (Fdbio, Hangzhou, China) for 20 min on ice and vibrated for 30 s. Protein content was quantitated with BCA Equal amounts of protein

(20 μg) were separated using sodium dodecyl sulfate–polyacrylamide gel electrophoresis (10 %. acrylamide) and transferred to a nitrocellulose membrane with an electrophoresis apparatus (Bio-Rad, West Berkeley, California, USA). Membranes were blocked in Tris-buffered saline with either 5 %. nonfat dry milk with 0.1 %. Tween-20. Blots were incubated with a primary antibody, anti-TJP1 or anti-occludin (1:200; Abclonal, Wuhan, China) overnight at 4 °C, washed three times with Tris-buffered saline containing 0.1 %. Tween-20, and incubated with HRP-conjugated goat anti-mouse or anti-rabbit antibodies (1:2000 – 1:4000; Abclonal, Wuhan, China) for 1 h at room temperature. ECL substrate solution was added on membranes before detected. Stripping buffer (Fdbio, Hangzhou, China) was used before switching different antibodies. GAPDH was used as reference. Proteins were detected using chemiluminescence (Bio-Rad, West Berkeley, California, USA). ImageJ (http://rsbweb.nih.gov/ij/) was used to analyze western blot signals. The density of each band was compared with the corresponding control band and normalized against GAPDH by densitometry.

Immunoflurescence of occludin expression

Monolayers of Caco-2 cells on EZSlide 8-well glass slides were rinsed with PBS and fixed with cold methanol at room temperature for 30 min. Nonspecific binding sites were blocked with 5 %. BSA in PBS for 10 min. Cells were incubated in PBS with primary antibody, anti-occludin (1:200 – 1:400; CST, Danvers, Massachusetts, USA) overnight at 4 °C. Cells were washed three times with PBS and incubated with goat-anti-mouse antibody (1:250 – 1:500; CST, Danvers, Massachusetts, USA) for 1 h at room temperature. Cells were washed three times with PBS and stained with Hoechst 33324 for 10 min. Cells were washed three times with PBS. Monolayers on slides were observed and analyzed with an Olympus IX73 inverted fluorescence microscope (Olympus, Tokyo, Japan).

Mast cells stimulation and β-hexosaminidase release assay

LAD-2 cells and MC-9 cells were individually transferred to Tyrode's solution (Jiandaoshou, Guangzhou, China) with A23187 calcium ionophore for 30 minutes for activation. At the end of the incubation, samples were centrifuged at 300 g for 5 minutes. Supernatants were collected to measure the β-hexosaminidase (β-Hex) release to assess LAD-2 cell activation. At the same time, equivalent cells were lysed with 0.5 %. Triton X-100, and total lysates were used to determine initial β-Hex content. Supernatants, total lysates, and controls were placed in 96-well plates (Corning, NY, USA). Substrate solutions (50 μl; p-nitrophenyl-N-acetyl-b-D-glucosaminide, 1.3 mg/ml in 0.1 mol/l citrate buffer, pH 4.5) were added to each well and incubated for 60 min at 37 °C (Jiandaoshou, Guangzhou, China). The reaction was stopped by adding 150 μl of 0.01 mol/l sodium carbonate/ sodium bicarbonate (pH 10). β-Hex release was assessed by measuring sample optical densities (OD) at 405 nm using a microplate spectrophotometer and expressed as a percentage ratio.

Histamine assay

A histamine assay kit (Telenbiotech, Guangzhou, China) was used to measure histamine release from LAD-2 cells or MC-9 cells. The ELISA assay was performed according to the manufacturer's instructions. After the assay, optical density (OD) was measured at 450 nm using a microplate spectrophotometer.

Activated LAD-2 cells viability and ROS levels in LAD-2 cells using flow cytometry

After treating with A23187, propofol, or NAC (ROS scavenger), LAD-2 cells in 6-well plates (1×10^6 cells/well) were centrifuged for 5 min at 1000 rpm. The supernatant was removed, and 1.5 ml PI staining solution was added to gently resuspend the cells. The cells were incubated for 5 min at room temperature. LAD-2 cells in 6-well plates (1×10^6 cells/well) were centrifuged for 5 min at 1000 rpm after the treatments. The supernatant was removed, and 1.5ml PBS with 10μM DHE (ROS dye) was added to resuspend and incubate samples gently for 60 min at 25 °C. Flow cytometry was performed with LSRFortessa™ (BD, Franklin Lakes, New Jersey, USA) by setting a blue laser (488 nm) and detection filters 610/20 nm band pass for PI or DHE with a low flow rate. The data were analyzed with FlowJo V10 (FlowJo, LLC, Ashland, Oregon, USA) to assess activated LAD-2 cell viability.

Flow cytometry of Ca²⁺ levels in LAD-2 cells

LAD-2 cells in 6-well plates (1×10^6 /well) were centrifuged for 5 min at 1000 rpm to remove the supernatant. 1.5 ml PBS with 4μM Fluo8, AM (Ca²⁺ probe; Jiandaoshou, Guangzhou, China) and 0.02 %. Pluronic F-127 (Jiandaoshou, Guangzhou, China) were added to gently resuspend and incubate for 20 min at room temperature. The Ca²⁺ level in LAD-2 cells was

measured using flow cytometry with a LSRFortessa™ equipped with a blue laser (488 nm) and detection filters of 535/30 nm band pass.

ERK1/2 phosphorylation assay

A cell-based ELISA assay kit (Abnova, Taoyuan, Taiwan, China) was used to measure the ERK1/2 phosphorylation level in Caco-2 cells. Caco-2 cells cultured in 96-well black side plates were used to perform ELISA according to manufacturer's instructions. Fluorescence intensity was measured at 535/590 nm for ERK1/2 and 360/450 nm for total proteins using a microplate spectrophotometer to assess the normalized ERK1/2 phosphorylation level.

Statistical analysis

Statistical analysis was performed using IBM SPSS Statistics 24 (IBM, New York, USA) and GraphPad Prism version 7.00 (GraphPad Software, Inc. La Jolla, California, USA). ImageJ (http://rsbweb.nih.gov/ij/) was used to analyze western blotting data. FlowJo V10 (FlowJo, LLC, Ashland, Oregon, USA) was used to analyze flow cytometry data. Results are expressed as mean ± s.e.m., and Student's t-test was used to assess statistical difference. $P<0.05$ was considered statistically significant.
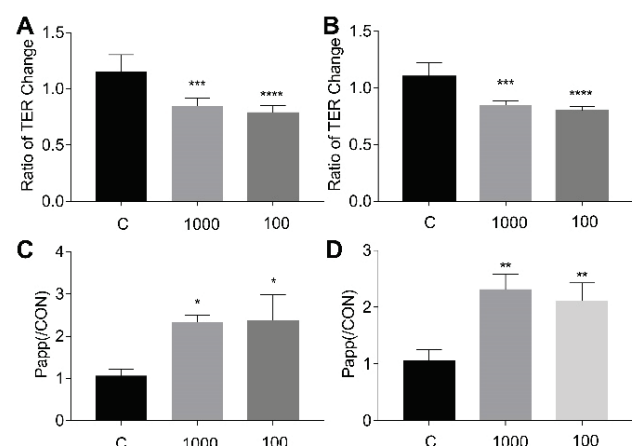
Results

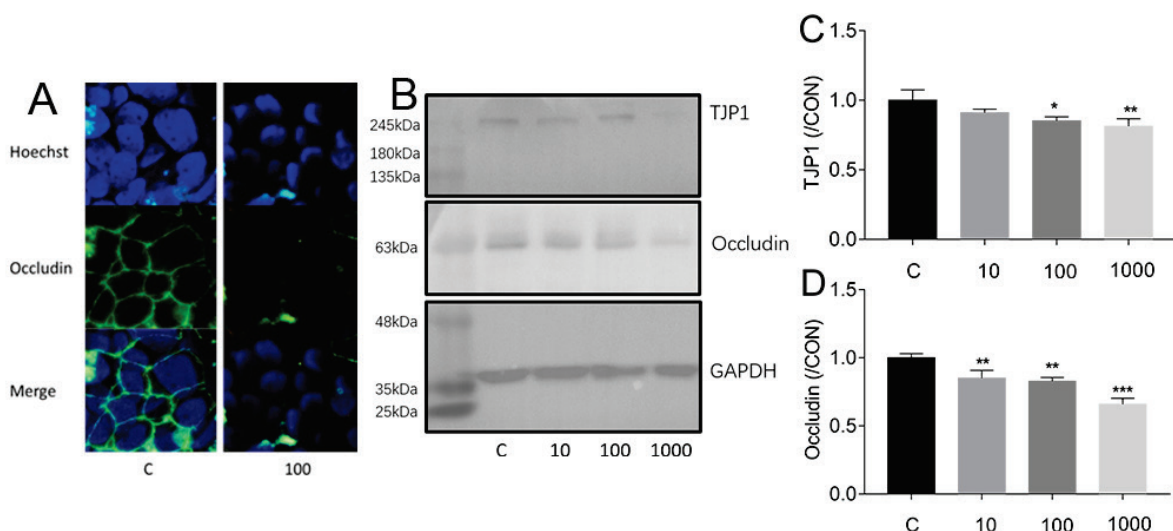*Tryptase directly interrupted intestinal barrier integrity via PAR-2*

We previously found that tryptase alone can result

in intestinal epithelial cell injury [5]. Here, we established a model of after mast cell activation and explored the direct role of tryptase in intestinal barrier function *in vitro*. As shown in Fig. 1, stimulation with 100-1000 ng/ml of tryptase for 4 h or 24 h significantly reduced the TER while increased Papp in Caco-2 cells. The samples stained by occludin further suggested that the intestinal barrier was disrupted by 100 ng/ml tryptase for 4 h (Fig. 2A). Moreover, incubating Caco-2 cells with 10, 100, or 1000 ng/ml of tryptase respectively displayed significant reductions in occludin and TJP1 proteins (Fig. 2B-D).
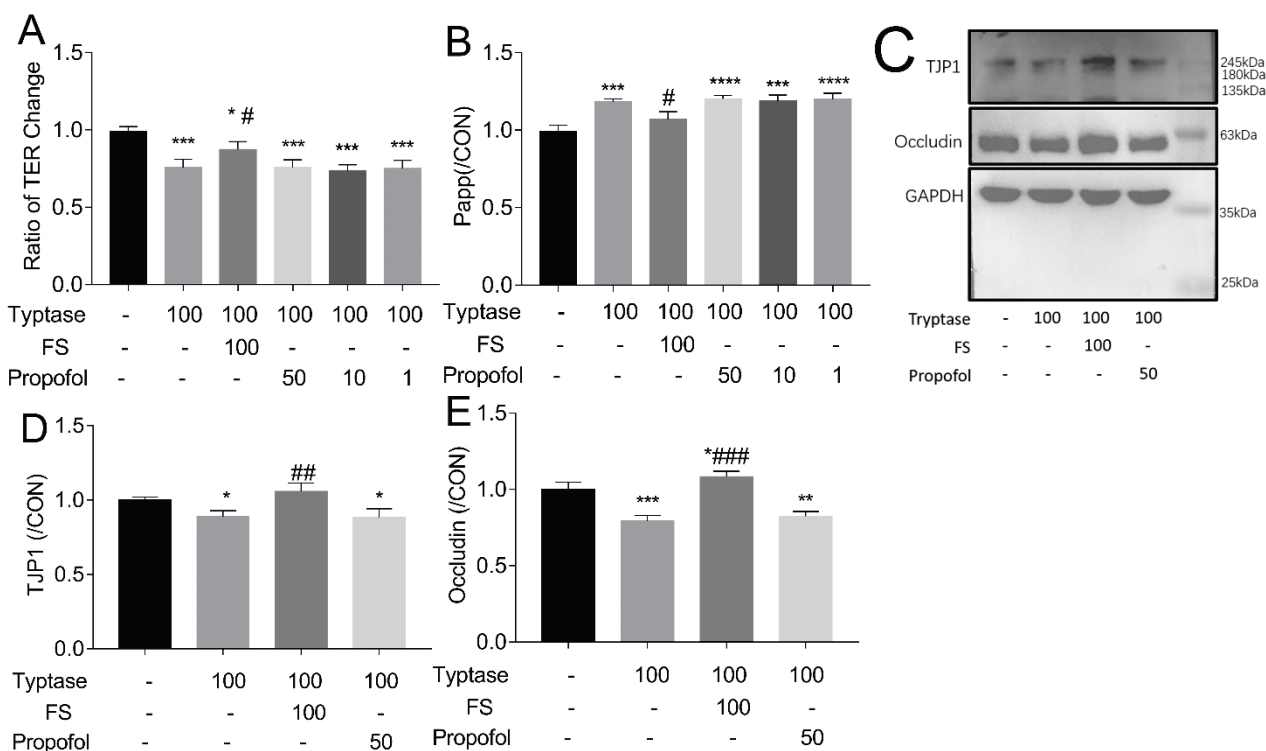
Next, we used a specific PAR-2 inhibitor (FSLLRY-NH2, FS) to explore the signal pathway of
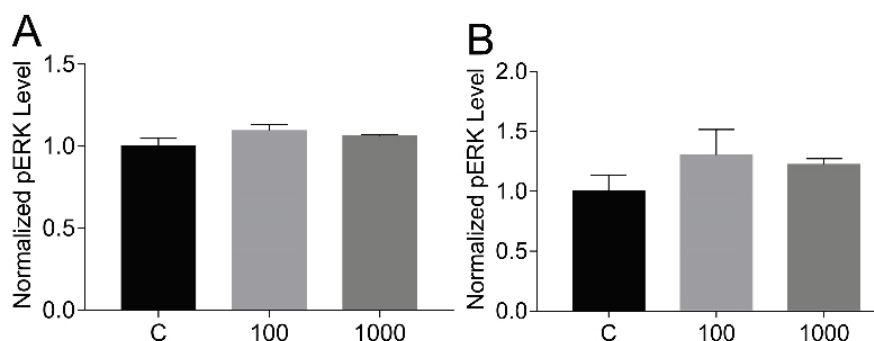

Fig. 1. Tryptase increased permeability of the Caco-2 monolayers. Change of TER and Papp in Caco-2 monolayers incubated with tryptase (ng/ml) for 4h (**AC**) or 24h (**BD**) compared to untreated controls. Results represent the mean ± SD, n=3. * versus control. * $P<0.05$, ** $P<0.01$, *** $P<0.001$, **** $P<0.0001$ (one-way ANOVA with Dunnett's *post hoc* test).

Fig. 2. Tryptase decreased expression of Caco-2 monolayers' junctional proteins. **A**) Expression of occludin in Caco-2 monolayers incubated with tryptase (ng/ml) for 4h. IF-IC, 400×. **BCD**) Expression of TJP1 and occludin in Caco-2 monolayers treated with tryptase (ng/ml) for 24h. Results represent the mean ± SD, n=3. * versus control. * $P<0.05$, ** $P<0.01$, *** $P<0.001$ (one-way ANOVA with Dunnett's *post hoc* test).

Fig. 3. FS alleviated tryptase-induced Caco-2 monolayers disruption but propofol cannot. **AB**) Change of TER and Papp in Caco-2 monolayers incubated with tryptase (ng/ml), tryptase + FS (µM), or tryptase + propofol (µM) for 4h compared to untreated controls. **CDE**) Expression of TJP1 and occludin in Caco-2 monolayers treated with tryptase (ng/ml), tryptase + FS (µM), or tryptase + propofol (µM) for 24h. Results represent the mean ± SD, n=3. * versus control, # versus tryptase (100ng/ml). * $P<0.05$, ** $P<0.01$, *** $P<0.001$, **** $P<0.0001$ (one-way ANOVA with Dunnett's *post hoc* test).

Fig. 4. Tryptase had no effect on the ERK1/2 phosphorylation of Caco-2 monolayers. Change of the normalized pERK level in Caco-2 monolayers incubated with tryptase (ng/ml) for 4h (**A**) or 24h (**B**) compared to untreated controls. Results represent the mean ± SD, n=3. * versus control, # versus tryptase (100ng/ml). * $P<0.05$ (one-way ANOVA with Dunnett's *post hoc* test).

tryptase, and as anticipated, treatment with 100 µM FS abrogated significant Papp increases as well as decreases in TER and Occludin and TJP1 protein expressions in the presence of challenge by 100 ng/ml tryptase stimulation (Fig. 3).

Propofol cannot protect against tryptase-induced intestinal barrier disruption

Propofol 1-50 µM did not block the tryptase-induced intestinal barrier disruption, because there was no statistical difference in TER and Papp between propofol treated and tryptase treated groups ($P>0.05$, Fig. 3), indicating post-treatment with propofol showed

no therapeutic effects on intestinal integrity after mast degranulation. A previous study demonstrated that tryptase-mediated IEC-6 cell injury occurred through the PAR-2/ERK signal pathway [5]. Propofol could inhibit ERK phosphorylation [8]. We next focused on the PAR-2/ERK signal pathway. However, there were no significant changes in ERK phosphorylation proteins after tryptase challenge in Caco-2 cells ($P>0.05$, Fig. 4).

Propofol attenuated mast cell degranulation-triggered increased intestinal permeability

A previous study revealed that mast cell activation aggravates remote organ injury induced by

small intestinal ischemia reperfusion injury [10]. To exclude the confounding factors affecting intestinal permeability in vivo, we established an *in vitro* model with co-culture of mast cells and Caco-2 cells. As expected, mast cell degranulation increased the intestinal permeability demonstrated by decreased TER and increased Papp in Caco-2 cells (Fig. 5A,B). This suggested the central role of mast cell degranulation in intestinal barrier disruption. Meanwhile, the increased intestinal permeability induced by mast cell degranulation was limited by propofol treatment (*P*<0.05, Fig. 5E-5F), indicating that propofol suppressed mast cell activation. Notably, mast cell degranulator A23187 has no effects on intestinal permeability changes (*P*>0.05, Fig. 5 I,J).
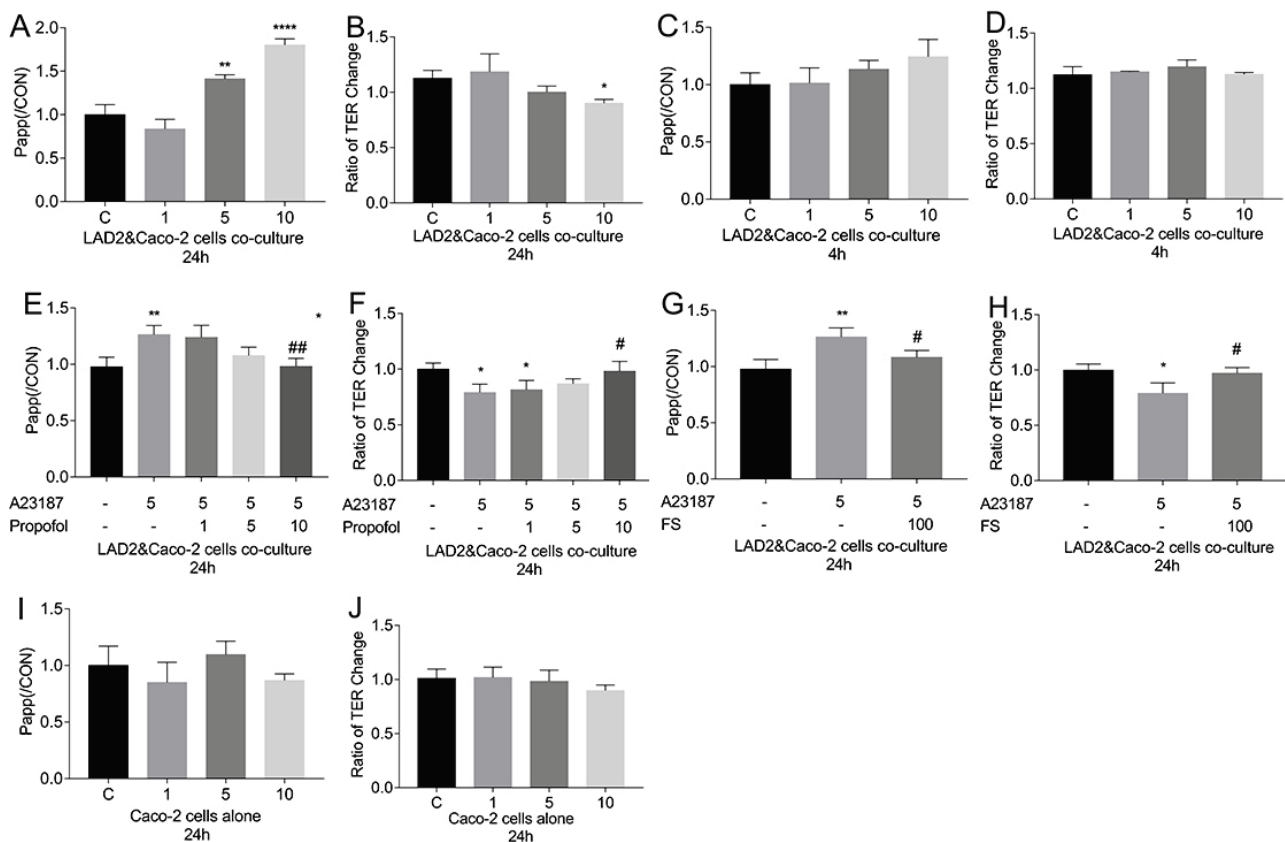
Propofol inhibited mast cell activation by A23187 via ROS/ Ca²⁺

Next, we investigated propofol's effects on mast cell degranulation. As shown in Fig. 6A-D, A23187 induced LAD2 cell and MC9 cell degranulation in a dose-dependent manner demonstrated by increased
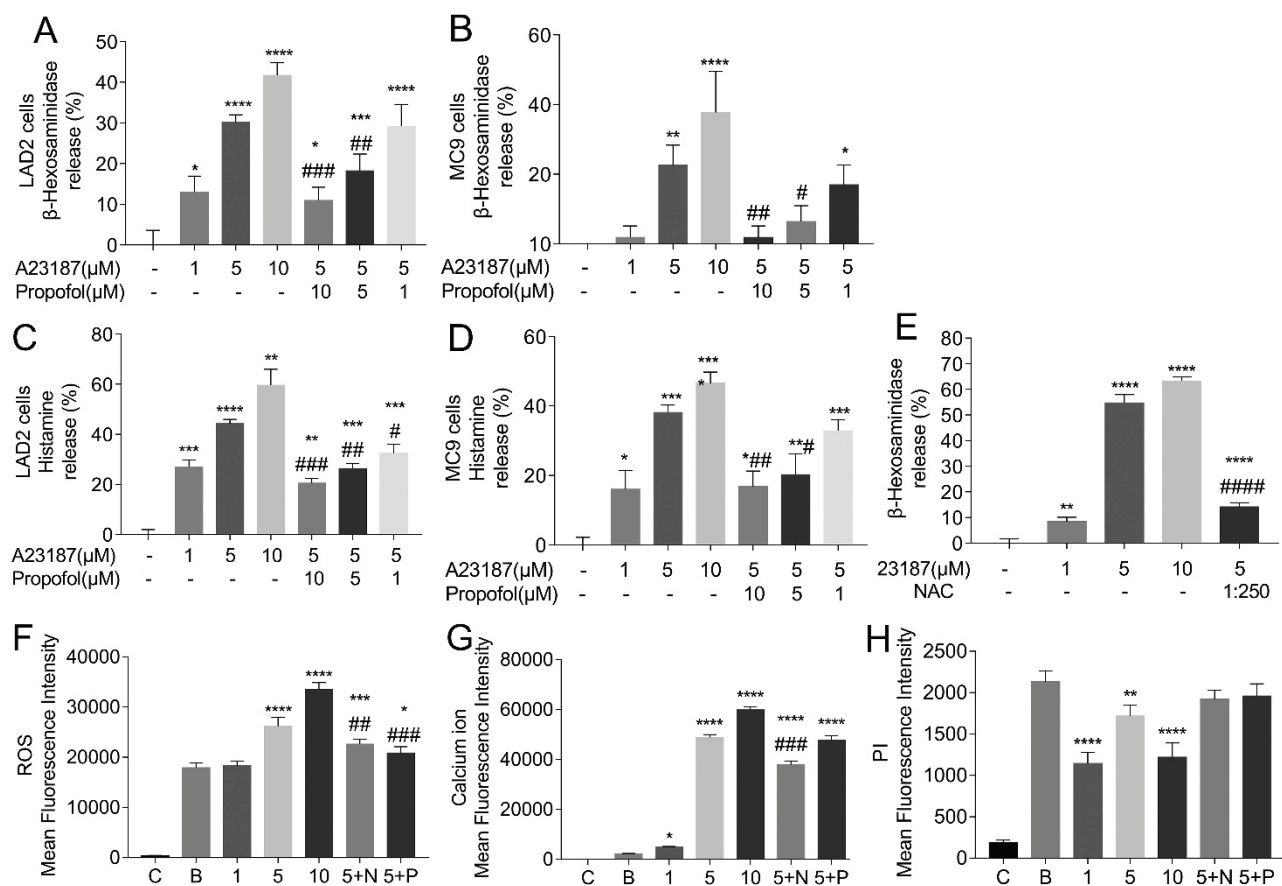
β-hexosaminidase and histamine levels. Propofol pretreatment dose-dependently blocked the activation of LAD2 and MC9 cell lines (*P*<0.05).

Because propofol provides anti-oxidative properties, we explored whether propofol inhibited mast cell activation via oxidative stress. As found in Fig. 6E, NAC, one of classical antioxidants, completely blocked mast cell degranulation. Propofol also showed the same effect (*P*<0.05). Furthermore, A23187 resulted in robust ROS increases determined using flow cytometry. Propofol and NAC similarly alleviated ROS increases (*P*<0.05, Fig. 6F). Moreover, A23187 dramatically induced calcium concentration increases in LAD2 cells. NAC significantly attenuated alterations in calcium concentration induced by A23187, and propofol slightly attenuated the alterations (Fig. 6G).

Notably, the selected concentration of A23187 here induced increased β-hexosaminidase and histamine via mast cell degranulation but not via mast cell apoptosis (Fig. 6H).

Fig. 5. Propofol and FS attenuated mast cell degranulation-triggered increased intestinal permeability. Change of Papp and TER in Caco-2 monolayers on the LAD2&Caco-2 co-culture model incubated with A23187 or A23187+propofol or A23187+FS compared with respective untreated controls. Results represent the mean±SD, n=3. * versus control, # versus A23187 (5µM). * *P*<0.05, ** *P*<0.01, **** *P*<0.0001 (one-way ANOVA with Dunnett's *post hoc* test).

Fig. 6. Propofol blocked the activation of mast cells and alleviated ROS increases. **ABCDE**) Stimulation of LAD2 and MC9 cells treated for 30min was evaluated by β-Hexosaminidase or histamine release. **FGH**) ROS level, Calcium ion level and PI level in LAD2 cells after 30 min-stimulation was detected. Data are presented as mean ± SD, n=3. * versus control (ABCDE) or blank (FGH), # versus A23187 (5μM). * $P<0.05$, ** $P<0.01$, *** $P<0.001$, **** $P<0.0001$ (one-way ANOVA with Dunnett's *post hoc* test). C: control; B: blank; 1: A23187 1μM; 5: A23187 5μM; 10: A23187 10μM; 5+N: A23187 5μM + NAC 1:250; 5+P: A23187 5μM + Propofol 10 μM in figure FGH.

Discussion

Here, we found that either mast cell activation or the released tryptase increased intestinal permeability *in vitro*, and this disruption was demonstrated by significant decreases in TER and increases in Papp. Propofol restored the altered intestinal barrier dysfunction by stimulated by mast cell activation but not by tryptase directly which was irrelevant to ERK phosphorylation. Further, propofol stabilized mast cell through ROS/Ca^{2+} signal pathway.

Propofol is one of widely used intravenous anesthetics for anesthesia induction and maintenance. Besides the role of general anesthesia, propofol in many fields displays preventive or protective benefits against ischemia reperfusion injury when treated either before or after ischemia [6], which is described pretreatment or post-treatment with propofol. Previous studies found that pretreatment with propofol can prevent mast cell

activation-exacerbated intestinal ischemia reperfusion injury in a rodent model [6], indicating that the benefits of pretreatment of propofol may through mast cell inhibition. Here, we found that propofol applied at clinically relevant concentrations stabilized two mast cell lines from degranulation. As expected, we also found that propofol maintained the intestinal barrier integrity interrupted by mast cell degranulation. Our results further provided the novel preventive benefits of propofol against intestinal permeability *in vitro* by inhibiting mast cells.

Because an increase in intracellular calcium concentration can trigger mast cell degranulation, we used A23187 to establish a model of mast cell activation *in vitro* according to a previous study [11]. We also found significant increases in β-hexosaminidase and histamine levels induced by A23187. Moreover, A23187 resulted in robust increases in ROS and Ca^{2+} concentrations detected by flow cytometry. Here, mast cell degranulation was completely blocked by propofol, which is in line with the

previous study[12], further suggesting the critical role of propofol in stabilizing Ca^{2+} induced mast cell degranulation. Rather, several lines of evidence recently reported that propofol can block superoxide production originating from NADPH oxidase *in vitro* [13]. We used NAC, a classical antioxidant, to investigate whether oxidative stress plays an important role in mast cell degranulation, and we found that either propofol or NAC similarly attenuated A23187-induced robust increases in superoxide production and Ca^{2+} levels. To our knowledge, our study is the first to show that propofol given at a sedative dosage significantly inhibited MC activation through ROS/Ca^{2+} *in vitro* although another study showed that propofol can inhibit mast cell exocytosis *in vitro* in a dose-dependent manner [7].

Mast cell activation plays a critical role in intestinal permeability alterations in vivo [14], and many factors can trigger mast cell activation during the period of ischemia[15]. Tryptase, mainly released from MC, accounts for more than 25 %. of the total MC protein [16]. In particular, tryptase is one of the main factors contributing to altered intestinal barrier permeability [9]. Previous studies have revealed that tryptase levels ranged from 9.3 to 525.0 ng/mg in the lower gastrointestinal tract after mast cell activation [17]. Thus, we adjusted tryptase in a range from 1 to 1000 ng/ml to explore its role in the intestinal barrier disruption process. As expected, 100-1000 ng/ml of tryptase directly interrupted barrier integrity, which was manifested by significant changes in TER, Papp, and tight junction proteins expression. Our findings further confirmed that tryptase plays a central role in intestinal barrier disruption.

If patients suffered hemorrhagic shock for emergent surgery, intestinal protective procedures like pretreatment would be unavailable while post-treatment should be advocated. Indeed, post-treatment with propofol has been shown to protective effects against hepatic ischemia reperfusion injury[18]. Caco-2 cells have been established as an *in vitro* intestinal barrier model because they exhibits a well differentiated brush border and tight junctions [19]. ZO-1 and occludin protein expression represent intestinal permeability of tight junction. It has been reported that knockdown of occludin expression enhances the permeability, and occludin-deficient animals develop a weakened gut barrier [20]. This suggests that the central role of occludin is to maintain integrity. Here, our results demonstrated that tryptase directly increases intestinal permeability by down-regulating ZO-1 and occludin

protein expression. Inhibiting PAR-2 can restore the tight junction proteins after the released tryptase exposure.

PAR-2 is highly expressed in the small intestinal mucosa. Our previous study revealed that tryptase stimulation can induce significant increases in PAR-2 protein expression in IEC-6 cells, and PAR-2 inhibitor FS had limited damage to IEC-6 cells triggered by 100-1000 ng/ml tryptase [5]. In agreement with the previous study, we also found here that tryptase-induced barrier disruption occurs via PAR-2 activation. Meanwhile, PAR-2 activation often results in subsequent downstream signal activation like mitogen-activated protein kinases (MAPK) pathways [21]. Groschwitz et al. demonstrated that chymase stimulation of Caco-2 cells induced significant increases in p38 and p44/42 (ERK1/2) activity [22]. Our previous study found that phosphorylated ERK protein was significantly increased and peaked 30 min after tryptase challenge [5]. However, we found here that tryptase induced disruption of Caco-2 cells in the absence of the ERK signal pathway, indicating the other potential signal pathway are involved.

A previous study reported that propofol can inhibit the ERK phosphorylation *in vitro* model of PMA-induced HOC1 production [8]. Propofol can reduce the pain response in an animal model of postoperative pain associated with the p38MAPK signal pathway [23]. Here, propofol failed to reduce tryptase-induced PAR-2 ERK phosphorylation. This discrepancy may be because Caco-2 is not related to the PAR-2/p38MAPK signaling pathway. Propofol has little influence in the tight junction changes and intestinal barrier disruption induced by tryptase, further indicating that post-treatment with propofol may through other mechanisms to protect intestinal barrier permeability after mast cell activation.

Several limitations of this study should be noted. First, the downstream MAPK pathways induced by PAR-2 activation include extracellular signal-regulated kinase 1/2 (ERK1/2), c-Jun N-terminal kinase (JNK), and p38 kinases. Only ERK1/2 was adjusted here because these kinases share the same signal pathways [24]. Second, inflammation and oxidative stress after mast cell activation contribute to intestinal injury, tryptase alone altered intestinal permeability cannot well represent the model of propofol post-treatment after mast cell activation.

Taken together, pretreatment, but not post-treatment, with propofol can restore intestinal barrier integrity induced by mast cell activation *via* ROS/Ca^{2+} signal pathway.

References

1. Bischoff SC. Mast cells in gastrointestinal disorders. Eur J Pharmacol 2016;778:139-45. https://doi.org/10.1016/j.ejphar.2016.02.018

2. Armacki M, Trugenberger AK, Ellwanger AK, Eiseler T, Schwerdt C, Bettac L, Langgartner D, Azoitei N, Halbgebauer R, Groß R, Barth T, Lechel A, Walter BM, Kraus JM, Wiegreffe C, Grimm J, Scheffold A, Schneider MR, Peuker K, Zeißig S, Britsch S, Rose-John S, Vettorazzi S, Wolf E, Tannapfel A, Steinestel K, Reber SO, Walther P, Kestler HA, Radermacher P, Barth TF, Huber-Lang M, Kleger A, Seufferlein T. Thirty-eight-negative kinase 1 mediates trauma-induced intestinal injury and multi-organ failure. J Clin Invest 2018;128:5056-5072. https://doi.org/10.1172/JCI97912

3. Bednarska O, Walter SA, Casado-Bedmar M, Ström M, Salvo-Romero E, Vicario M, Mayer EA, Keita ÅV. Vasoactive Intestinal Polypeptide and Mast Cells Regulate Increased Passage of Colonic Bacteria in Patients With Irritable Bowel Syndrome. Gastroenterology 2017;153:948-960.e3. https://doi.org/10.1053/j.gastro.2017.06.051

4. Albert-Bayo M, Paracuellos I, González-Castro AM, Rodríguez-Urrutia A, Rodríguez-Lagunas MJ, Alonso-Cotoner C, Santos J, Vicario M. Intestinal Mucosal Mast Cells: Key Modulators of Barrier Function and Homeostasis. Cells 2019;8:135. https://doi.org/10.3390/cells8020135

5. Li S, Guan J, Ge M, Huang P, Lin Y, Gan X. Intestinal mucosal injury induced by tryptase-activated protease-activated receptor 2 requires β-arrestin-2 *in vitro*. Mol Med Rep 2015;12:7181-7. https://doi.org/10.3892/mmr.2015.4325

6. Zhao W, Zhou S, Yao W, Gan X, Su G, Yuan D, Hei Z. Propofol prevents lung injury after intestinal ischemia-reperfusion by inhibiting the interaction between mast cell activation and oxidative stress. Life Sci 2014;108:80-7. https://doi.org/10.1016/j.lfs.2014.05.009

7. Fujimoto T, Nishiyama T, Hanaoka K. Inhibitory effects of intravenous anesthetics on mast cell function. Anesth Analg 2005;101:1054-9. https://doi.org/10.1213/01.ane.0000166955.97368.80

8. Chen M-S, Lin W-C, Yeh H-T, Hu C-L, Sheu S-M. Propofol specifically reduces PMA-induced neutrophil extracellular trap formation through inhibition of p-ERK and HOCl. Life Sci 2019;221:178-186. https://doi.org/10.1016/j.lfs.2019.02.030

9. Wilcz-Villega EM, McClean S, O'Sullivan MA. Mast cell tryptase reduces junctional adhesion molecule-A (JAM-A) expression in intestinal epithelial cells: implications for the mechanisms of barrier dysfunction in irritable bowel syndrome. Am J Gastroenterol 2013;108:1140-51. https://doi.org/10.1038/ajg.2013.92

10. Zhao W, Huang X, Han X, Hu D, Hu X, Li Y, Huang P, Yao W. Resveratrol Suppresses Gut-Derived NLRP3 Inflammasome Partly through Stabilizing Mast Cells in a Rat Model. Mediators Inflamm 2018;2018:6158671. https://doi.org/10.1155/2018/6158671

11. Kim D-Y, Kang T-B, Shim D-W, Sun X, Han J-W, Ji Y-E, Kim T-J, Koppula S, Lee K-H. Emodin attenuates A23187-induced mast cell degranulation and tumor necrosis factor-α secretion through protein kinase C and IκB kinase 2 signaling. Eur J Pharmacol 2014;723:501-6. https://doi.org/10.1016/j.ejphar.2013.09.066

12. Yi Z, Yi Z, Huang KAI, Cao Y, Xiao C, Li Y, Lu Q, Zhao S, Luo W, Liu G. Propofol attenuates mast cell degranulation via inhibiting the miR-221/PI3K/Akt/Ca^{2+} pathway. Exp Ther Med 2018;16:1426-1432. https://doi.org/10.3892/etm.2018.6317

13. Chen X, Zhou X, Yang X, Zhou Z, Lu D, Tang Y, Ling Z, Zhou L, Feng X. Propofol protects against H_2O_2-Induced oxidative injury in differentiated PC12 cells via inhibition of Ca^{2+}-dependent NADPH oxidase. Cell Mol Neurobiol 2016;36:541-551. https://doi.org/10.1007/s10571-015-0235-1

14. Wouters MM, Vicario M, Santos J. The role of mast cells in functional GI disorders. Gut 2016;65:155-68. https://doi.org/10.1136/gutjnl-2015-309151

15. He Z, Ma C, Yu T, Song J, Leng J, Gu X, Li J. Activation mechanisms and multifaceted effects of mast cells in ischemia reperfusion injury. Exp Cell Res 2019;376:227-235. https://doi.org/10.1016/j.yexcr.2019.01.022

16. Pejler G, Rönnberg E, Waern I, Wernersson S. Mast cell proteases: multifaceted regulators of inflammatory disease. Blood 2010;115:4981-90. https://doi.org/10.1182/blood-2010-01-257287

17. Hagel AF, deRossi T, Zopf Y, Konturek P, Dauth W, Kressel J, Hahn EG, Raithel M. Mast cell tryptase levels in gut mucosa in patients with gastrointestinal symptoms caused by food allergy. Int Arch Allergy Immunol 2013;160:350-5. https://doi.org/10.1159/000341634

18. Ma H, Liu Y, Li Z, Yu L, Gao Y, Ye X, Yang B, Li H, Shi J. Propofol protects against hepatic ischemia reperfusion injury via inhibiting Bnip3-mediated oxidative stress. Inflammation 2021;44:1288-1301. https://doi.org/10.1007/s10753-021-01416-z

19. Haines RJ, Beard RS, Chen L, Eitnier RA, Wu MH. Interleukin-1β Mediates β-Catenin-Driven downregulation of claudin-3 and barrier dysfunction in Caco2 Cells. Dig Dis Sci 2016;61:2252-61. https://doi.org/10.1007/s10620-016-4145-y

20. Saitou M, Furuse M, Sasaki H, Schulzke JD, Fromm M, Takano H, Noda T, Tsukita S. Complex phenotype of mice lacking occludin, a component of tight junction strands. Mol Biol Cell 2000;11:4131-42. https://doi.org/10.1091/mbc.11.12.4131

21. Rothmeier AS, Ruf W. Protease-activated receptor 2 signaling in inflammation. Semin Immunopathol 2012;34:133-49. https://doi.org/10.1007/s00281-011-0289-1

22. Groschwitz KR, Wu D, Osterfeld H, Ahrens R, Hogan SP. Chymase-mediated intestinal epithelial permeability is regulated by a protease-activating receptor/matrix metalloproteinase-2-dependent mechanism. Am J Physiol Gastrointest Liver Physiol 2013;304:G479-89. https://doi.org/10.1152/ajpgi.00186.2012

23. Wong SS-C, Sun L, Qiu Q, Gu P, Li Q, Wang X-M, Cheung CW. Propofol attenuates postoperative hyperalgesia via regulating spinal GluN2B-p38MAPK/EPAC1 pathway in an animal model of postoperative pain. Eur J Pain 2019;23:812-822. https://doi.org/10.1002/ejp.1349

24. Darling NJ, Cook SJ. The role of MAPK signalling pathways in the response to endoplasmic reticulum stress. Biochim Biophys Acta 2014;1843:2150-63. https://doi.org/10.1016/j.bbamcr.2014.01.009